Supporting Information for

Multivalent Recognition of Lectins by Glyconanoparticle Systems

Eugene Mahon,[a] *Teodor Aastrup,*[b] *Mihail Barboiu*[*, a]

[a]Institut Européen des Membranes, Adaptive Supramolecular Nanosystems Group, ENSCM-UMII-CNRS UMR-5635, Place Eugène Bataillon, CC 047, F-34095, Montpellier, France.

[b]Attana AB, Björnnäsvägen 21, S-11347 Stockholm, Sweden,

E-mail : mihai.barboiu@iemm.univ-montp2.fr

Our general approach relied on the following synthetic or analytical steps:

a) Preparation and characterisation of gold glyconanoparticle library suitable for QCM technique (i.e. fully water/buffer soluble, stable);

b) Optimisation of QCM running experimental conditions (buffer, flow speed, surface properties)

c) Investigation of lectin (ConA) layer formation on QCM electrode;

d) Investigation of the specificity and avidity of glyconanoparticle with adsorbed protein layers.

Materials and Methods

All of the following materials used were obtained from commercial sources and used without further purification. Gold (III) chloride trihydrate (CAS : 16961-25-4), 2-oleoyl-1-palmitoyl-sn-glycero-3-phosphocholine (CAS : 26853-31-6), 2-[2-(2-chloroethoxy)ethoxy]ethanol (CAS: 5197-62-6), sodium citrate tribasic dihydrate, borontrifluoride-diethyletherate (CAS: 109-63-7), 1-tetradecyne (CAS: 765-10-6), sodium azide (CAS: 26628-22-8), tetrabutylammonium hydrogensulfate (CAS: 32503-27-8), hydrogen bromide in acetic acid, thioacetic acid (CAS: 88620), copper(II) sulfate pentahydrate (CAS: 7758-99-8), ascorbic acid sodium salt (CAS: 134-03-2), 1-octadecanethiol (CAS: 2885-00-9), methyl-alpha-D-glucopyrannoside (CAS : 97-30-3), mannan (CAS: 9036-88-8) were all purchased from either Sigma-Aldrich or Fluka. Analytical TLC was performed on silica gel 60-F_{254} (Whatman) with detection by immersion in 5% methanolic H_2SO_4 followed by charring or by fluorescence. Column chromatography was performed with silica gel 60 A C.C 70-200 μm. 2-(2-(2-mercaptoethoxy) ethoxy)ethanol (16) was prepared following a known protocol. [1]

^1H and ^{13}C NMR spectra were recorded on an ARX 300 MHz Bruker spectrometer in $CDCl_3$ and CD_3CN with the use of the residual solvent peak as reference. Mass spectrometric studies were performed in the positive ion mode using a quadrupole mass spectrometer (Micromass, Platform II). Samples were continuously introduced into the mass spectrometer through a Waters 616HPLC pump. The temperature (60°C) and the extraction cone voltage (V_c=5-10V) were usually set to avoid fragmentations. SEM images were obtained with a Hitachi S-4500 apparatus (0.5-30 kV). The TEM micrographs were obtained with a High Resolution transmission electron microscopy (HRTEM) JEOL 2010FEG apparatus, working with an accelerating voltage of 200 kV and a point resolution of 2.0 Å.

QCM measurements were performed using the A100 instrument from Attana Biosensors. The experiments were run in the continuous-flow QCM system at a flow rate of 20 μL/min. The experiments were performed in a Tris buffer at pH 7.4. All species were dissolved in this medium so as to ensure buffer effects be kept to a minimum. SEM images were obtained with a Hitachi S-4500 apparatus (0.5-30 kV). The TEM micrographs were obtained with a High Resolution transmission electron microscopy

(HRTEM) JEOL 2010FEG apparatus, working with an accelerating voltage of 200 kV and a point resolution of 2.0 Å. Dynamic light scattering measurements were performed with the Cordouan SL135. SEM images were obtained with a Hitachi S-4500 apparatus (0.5-30 kV).

Glycoligands Preparation

The ligands were prepared in a three step synthesis from the simple sugars. Peracetylation was followed by Lewis acid catalysed glycosylation with $BF_3.Et_2O$ [2-4S] giving the α-anomer in the case of mannose peracetate due to the neighbouring group participation and anomeric effect and β-anomer for the other peracetates as it to be expected due to neighbouring C2 acetoxy group participation.[5S]

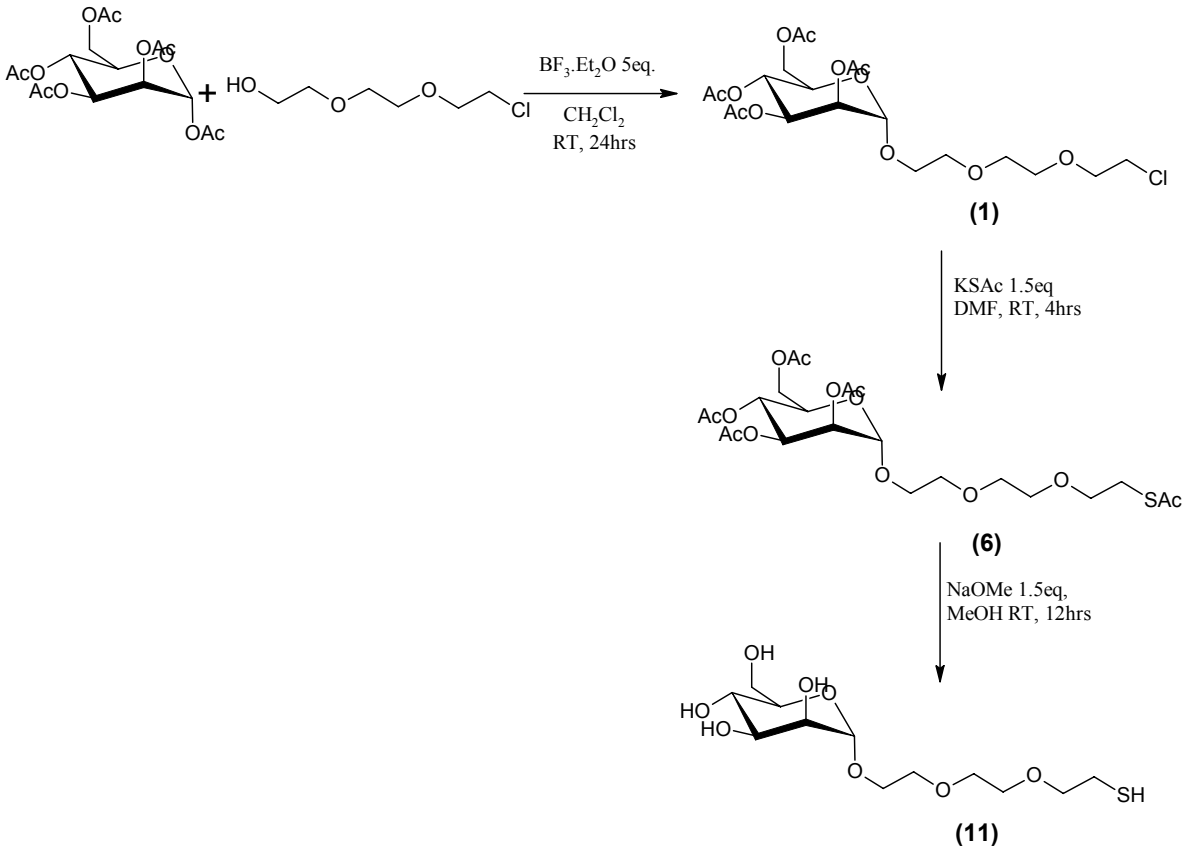

Figure 1S Reaction scheme for preparation of α-D-Mannopyranoside2-[2-(2-mercaptoethoxy) ethoxy]ethyl.

The chloroglycol glycosides thus prepared were then treated with potassium thioacetate in DMF to give the thioacetates in high yield followed by deacetylation with MeONa in MeOH with some presence of disulfides also in the products which are equally suitable for the next step of glyconanoparticle preparation.

General Synthesis of D-Glycopyranoside, 2-[2-(2-chloroethoxy)ethoxy]ethyl, 2,3,4,6-tetraacetates.

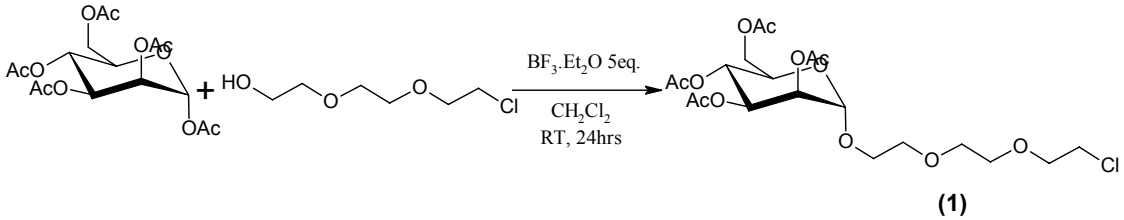

Figure 2S Glycosylation Step.

7.74 ml of $BF_3.Et_2O$ (min 46.5% w/v BF_3) (3.6 g, 5 equiv., 25.6 mmol) was added dropwise to a solution of 2-[2-(2-chloroethoxy)ethoxy]ethanol (1.3 g, 1.5 eq., 7.68 mmol) and the peracetylated carbohydrates (1 eq., 5.12 mmol) in dry dichloromethane (25 ml) stirring at 0 °C. The mixture was allowed to warm to RT and then stirred for a further 24 hrs in the case of the mannoside preparation and 72 hours for the other glycosides. The product was extracted with dichloromethane and washed with $NaHCO_3$ sat. (x3) and then dried over Na_2SO_4. The product was purified by flash column chromatography using EtOAc/Hexane as eluent (1:1) to afford the glycosylated products in the form of pale residues.

α-D-Mannopyranoside, 2-[2-(2-chloroethoxy)ethoxy]ethyl, 2,3,4,6-tetraacetate ***(1)***

Yield 45%. ^{1}HNMR(300MHz, $CDCl_3$, 25°C): δ=1.98 (s, 3H, CH_3CO), δ2.05 (s, 3H, CH_3CO), δ2.12 (s, 3H, CH_3CO), δ2.16 (s, 3H, CH_3CO), 3.6-3.76 (m, 12H, OCH_2CH_2O) 4.04-4.07 (m, 1H, H-6), 4.1 (dd, 1H, J = 12.3, 2.5Hz, H-6), 4.3 (dd, 1H, J= 12.3, 5.1 Hz, H-5), 4.88 (d, J= 1.5 Hz,1H, H-1), 5.27 (m, 2H, H-2, H-3), 5.36 (dd, 1H, J= 12.3, 3.3 Hz, H-4). ^{13}C NMR (300MHz, $CDCl_3$): δ=20.6, 20.7, 20.8, 21.0 (4s, 4×CH$_3$CO), 42.255 (CH_2Cl), 62(C6), 65.7, 66.9, 68.58, 69.11, (4s, C-2 to C-5), 67.94, 69.56, 70.17, 70.24, 70.90 (5s, 5×CH$_2$O), 97.22(C1), 169.2, 169.35, 169.5, 170.1 (4s, 4×CH$_3$$C$O).

β-D-Glucopyranoside, 2-[2-(2-chloroethoxy)ethoxy]ethyl, 2,3,4,6-tetraacetate **(2)**

Yield 40%. ^{1}HNMR(300MHz, $CDCl_3$, 25°C): δ=2.0 (s, 3H, CH_3CO), 2.019 (s, 3H, CH_3CO), 2.04 (s, 3H, CH_3CO), 2.08 (s, 3H, CH_3CO), 3.6-3.8 (m, 12H, OCH_2CH_2O), 3.9-4.0 (m, 1H, H-6), 4.1 (m, 1H, H-6), 4.26 (dd, 1H, J= 12.3, 5.1 Hz, H-5), 4.6 (d, 1H, J= 8 Hz, H-1), 4.98 (dd, 1H, J= 9.3, 8 Hz, H-2), 5.1 (dd, 1H, J= 9.3, 9.3 Hz, H-3), 5.2 (dd, 1H, J= 9.3, 9.3 Hz, H-4). ^{13}C NMR (300MHz, $CDCl_3$): δ=20.1, 20.12, 20.18, 20.25 (4s, 4×CH$_3$CO), 42.25 (CH_2Cl), 61.47 (C6), 67.93, 68.56, 71.3,72.34 (4s, C-2 to C-5), 69.91, 70.18, 70.79, 70.88, (4s, 6×CH$_2$O), 100.33 (C1),168.87, 168.92, 169.78, 170.18 (4s,4×CH$_3$$C$O).

β-D-Galactopyranoside, 2-[2-(2-chloroethoxy)ethoxy]ethyl, 2,3,4,6-tetraacetate **(3)**

Yield 31%. ^{1}HNMR (300MHz, $CDCl_3$, 25°C): δ=1.98 (s, 3H, CH_3CO), 2.04 (s, 3H, CH_3CO), 2.05 (s, 3H, CH_3CO), 2.14 (s, 3H, CH_3CO), 3.6-3.8 (m, 12H, OCH_2CH_2O), 3.9-4.0 (m, 1H, H-6), 4.1 (m, 1H, H-6), 4.55 (d, 1H, *J*= 8 Hz, H-1), 5.0 (dd, 1H, *J*= 10, 3 Hz, H-3), 5.2 (dd, *J*= 10, 8 Hz, 1H, H-2) 5.4 (d, 1H, *J*= 3 Hz, H-4). ^{13}C NMR (300MHz, $CDCl_3$): δ=20.09, 20.17, 20.28, 20.54 (4s, 4×*C*H_3CO), 42.27(CH_2Cl), 60.8(C6), 66.58, 68.33,68.57 70.89 (4s, C-2 to C-5), 69.65, 69.9, 70.18, 70.42 (4s, 6×CH_2O), 100.87(C1),168.98, 169.66,169.76, 170.09 (4s, 4×CH_3*C*O).

β-D-Glucopyranoside, 2-[2-(2-chloroethoxy)ethoxy]ethyl4-O-(2,3,4,6-tetra-O-acetyl-β-D-galactopyranosyl)- , 2,3,6-triacetate **(4)**

Yield 35%. ^{1}HNMR (300MHz, $CDCl_3$, 25°C): δ=1.97(s, 3H), 2.05(m, 12H), 2.12(s, 3H) 2.16 (s, 3H)7×CH_3CO, 3.6-3.8 (m, 12H, OCH_2CH_2O), 3.8-3.95 (m, 2H, CH), 4.05-4.15(m, 4H, CH2), 4.47-4.58 (m, 2H, CH2), 4.56 (d, 2H, *J*=7.8, CH), 4.89 (t, 1H, CH), 4.95 (dd, 1H, *J*= 10.5, 3.3Hz, CH), 5.1 (dd, 1H, *J*=10.5, 7.8, H-2,), 5.195 (t, 1H, *J*= 9.3 Hz, CH) 5.34 (d, 1H, *J*= 3.3 Hz, CH).

β-D-Glucopyranoside, 2-[2-(2-chloroethoxy)ethoxy]ethyl 4-O-(2,3,4,6-tetra-O-acetyl-α-D-glucopyranosyl)-, 2,3,6-triacetate **(5)**

Yield 29%. ^{1}HNMR (300MHz, $CDCl_3$, 25°C): δ=1.95-2.09 (m, 18H), δ2.1 (s, 3H), 2.14 (s, 3H)7×CH_3CO, 3.6-3.8(m, 12H), 3.9-4 (m, 3H, CH), 4.05(dd, 1H, *J*= 12,3 Hz, CH), 4.25 (m, 2H, CH2), 4.49 (dd, 1H, *J*=12, 3Hz, CH), 4.63 (d, 1H, *J*= 7.8Hz, CH), 4.8-4.9 (m, 2H, CH), 5.05 (t, 1H, *J*= 10), 5.25 (t, 1H, *J*= 9 Hz, CH) 5.35 (t, *J*= 10 Hz,1H, CH), 5.4 (d, 1H, *J*= 3.9 Hz, CH).

General Synthesis of α-D-Mannopyranoside, 2-[2-(2 (acetylthio)ethoxy)ethoxy] ethyl, 2,3,4,6-tetraacetate.

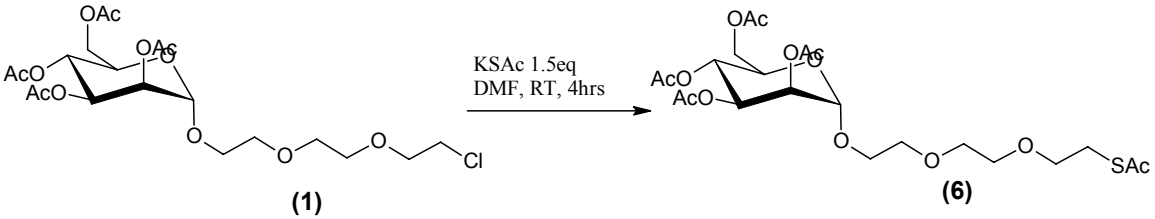

(1) **(6)**

Figure 3S Thioacetate Substitution.

α-D-Mannopyranoside 2-[2-(2-chloroethoxy)ethoxy]ethyl,2,3,4,6-tetraacetate (200 mg, 0.4 mmol, 1 eq) and potassium thioacetate (138 mg, 0.6mmol, 3 eq.) were taken and dissolved in DMF (10 ml). This solution was then stirred at room temperature for 4 hrs. Ethyl acetate (40 ml) was then added to the

reaction mixture which was then washed with H_2O(x2), $NaHCO_3$ and finally saturated NaCl. This organic phase was then evaporated off leaving a colourless oil.

α-D-Mannopyranoside, 2-[2-(2-(acetylthio)ethoxy)ethoxy]ethyl, 2,3,4,6-tetraacetate **(6)**

Yield 82%. ^{1}HNMR (300MHz, $CDCl_3$, 25°C): δ=1.95 (s, 3H), 2.01 (s, 3H), 2.06 (s, 3H), 2.12 (s, 3H) 4×C*H*$_3$CO, 2.3 (s, 3H, C*H*$_3$COS), 3.1(tr, 2H, *J*= 6Hz, CH_2CH_2S), 3.55-3.76(m, 10H), 4.04-4.07 (m, 1H, H-6), 4.1 (dd, 1H, *J*= 12.3, 2.4Hz, H-6), 4.25 (dd, *J*= 12.3, 1H, 5.1 Hz, H-5), 4.88 (d, 1H, *J*= 1.5 Hz, H-1), 5.23 (m, 2H, H-2, H-3), 5.36 (dd, 1H, *J*= 12.3, 3.0 Hz, H-4). ^{13}C NMR (300MHz, $CDCl_3$): δ=20.6, 20.7, 20.8, 21.0 (4s, 4×*C*H_3CO), 28.28(CH_2CH_2S), 29.97 (*C*H_3COS), 42.255 (*C*H_2Cl), 62(C6), 65.7, 66.9, 68.58, 69.11, (4s, C-2 to C-5), 67.94, 69.56, 70.17, 70.24, 70.90, (5s, 5×CH_2O), 97.22 (C1) 169.2, 169.35, 169.5, 170.1 (4s,4×CH_3CO), 194.84 (CH_3*C*OS). Lit: [6S]

β-D-Glucopyranoside, 2-[2-(2-(acetylthio)ethoxy)ethoxy]ethyl, 2,3,4,6-tetraacetate **(7)**

Yield 86%. ^{1}HNMR (300MHz, $CDCl_3$, 25°C): δ 1.988 (s, 3H), 2.01 (s, 3H), 2.044 (s, 3H), 2.09 (s, 3H) 4×C*H*$_3$CO 2.35 (s, 3H, C*H*$_3$COS), 3.1(tr, 2H, *J*= 6Hz, CH_2CH_2S), 3.55-3.7 (m, 12H, OCH_2CH_2O), 3.9 (m, 1H, H-6), 4.1 (dd, 1H, *J*= 12.3, 2.3 Hz, H-6)), 4.25 (dd, 1H, *J*= 12.3, 4.8 Hz, H-5), 4.61 (d, *J*= 8 Hz, 1H, H-1), 5.01 (dd, 1H, , *J*= 9, 8.1 Hz H-2), 5.08 (t, 1H, *J*= 9.5 Hz, H-3), 5.2 (tr, 1H, *J*= 9.5 Hz, H-4). ^{13}CNMR (300MHz, $CDCl_3$): δ=20.1, 20.12, 20.18, 21.25 (4s, 4×*C*H_3CO), 28.28(CH_2CH_2S), 30.07 (CH_3COS), 61.48(C6), 67.93, 68.56, 71.3, 72.34 (4s, C-2 to C-5), 69.91, 70.18, 70.79, 70.88, (4s, 6×OCH_2CH_2O), 100.35 (C1), 168.87, 168.92,169.78, 170.18 (4s,4×CH_3CO), 194.03 (CH_3*C*OS) .

β-D-Galactopyranoside, 2-[2-(2-(acetylthio)ethoxy)ethoxy]ethyl, 2,3,4,6-tetraacetate **(8)**

Yield 78%. ^{1}HNMR(300MHz, $CDCl_3$, 25°C): δ=1.98 (s, 3H), 2.04(s, 3H), 2.05(s, 3H), 2.14 (s, 3H) 4×C*H*$_3$CO, 2.35 (s, 3H), C*H*$_3$COS, 3.08(tr, 2H, *J*= 6Hz, CH_2CH_2S), 3.55-3.76 (m, 12H), 3.9-4.0 (m, 2H, H-6), 4.1 (m, 1H, H-5), 4.55 (d, 1H, *J*= 8 Hz, H-1), 5.0 (dd, 1H, *J*= 10, 3 Hz, H-3), 5.2 (dd, 1H, *J*= 10, 8 Hz, H-2) 5.4 (app d, 1H, *J*= 3 Hz, H-4). ^{13}CNMR (300MHz, $CDCl_3$): δ=20.09, 20.17, 20.28, 20.54 (4s, 4×*C*H_3CO), 27.4 (CH_2CH_2S), 29.7 (CH_3COS), 60.8(C6), 66.58, 68.33, 68.57, 70.89 (4s, C-2 to C-5), 69.65, 69.9, 70.18, 70.42 (4s, 6×CH_2O), 100.87(C1), 168.97, 169.65, 169.76, 169.89 (4s,4×CH_3CO), 194.03 (CH_3*C*OS). Lit: [6S]

β-D-Glucopyranoside, 2-[2-(2-(acetylthio)ethoxy)ethoxy]ethyl 4-O-(2,3,4,6-tetra-O-acetyl-β-D-galactopyranosyl)-, 2,3,6-triacetate **(9)**

Yield 81%. ^{1}HNMR(300MHz, $CDCl_3$, 25°C): δ=1.855 (s, 3H), 1.935 (s, 3H), 1.941 (m, 6H), 1.955 (s, 3H), 2.014 (s, 3H), 2.046 (s, 3H) 7×C*H*$_3$CO, 2.23 (s, 3H, C*H*$_3$COS), 2.92(tr, *J*= 6.3Hz, 2H, CH2S), 3.6-

3.8 (m, 12H), 3.85 (m, 2H, CH), 4.01 (m, 2H, CH) 4.38(dd, 1H, *J*= 1.8Hz , 12.6Hz, CH), 4.42 (d, 1H, *J*=7.8Hz, CH), 4.49 (d, 1H, *J*= 7.8Hz, CH), 4.78 (dd, 1H, *J*= 7.8hz , 9.3Hz, CH), 4.86 (dd, 1H, *J*= 10.5, 3.3Hz, CH), 4.9 (dd, 1H, *J*= 10.5, 7.8Hz, CH), 5.1 (t, 1H, *J*H = 9.3 Hz, CH), 5.24 (d, 1H, *J*= 3.6 Hz, CH). ^{13}C NMR (300MHz, $CDCl_3$): 19.920, 20.049, 20.049, 20.079, 20.130, 20.22, 20.27 (7 x CH_3CO), 28.212 (CH_2CH_2S), 29.982 (CH3COS), 60.298 (C6Gal), 61.526 (C6Glu), 66.131 (C-4Gal), 68.497, 68.580 (CH2), 69.139 (C-2Gal), 69.72, 70.28, 70.07 (CH2) 70.409 (C-5Gal), 70.77 (C-3Gal), 71.1 (C-2Glu), 72.0 (C-5Glu), 72.271 (C-3Glu), 75.75 (C-4Glu), 100.01 (C-1Gal), 100.458 (C-1Glu), 168.452, 168.99, 169.12, 169.37, 169.51, 169.68, 169.7 (CH_3CO), 194.7 (CH_3CS).

β-D-Glucopyranoside, 2-[2-(2-(acetylthio)ethoxy)ethoxy]ethyl 4-O-(2,3,4,6-tetra-O-acetyl-α-D-glucoopyranosyl)-, 2,3,6-triacetate **(10)**

Yield 85%. ^{1}HNMR(300MHz, $CDCl_3$, 25°C): *δ*=1.966 (s, 6H), 2.006 (s, 3H), 2.009 (s, 3H), 2.028 (s, 3H), 2.087 (s, 3H), 2.12 (s, 3H) (7×CH_3CO), 2.32 (s, 3H, CH3COS) 3.08 (tr, 2H, *J*= 6.3Hz, CH_2CH_2S), 3.6 (m, 8H, OCH_2CH_2O), 3.95 (m, 2H, CH), 3.8-3.9 (m, 2H), 4.2 (m, 2H, CH), 4.47 (dd, 1H, *J*= 12Hz, 3Hz, CH), 4.61 (d, 1H, *J*= 8 Hz, CH), 4.8 (m, 2H, CH) , 5 (tr, 1H, *J*= 10 Hz, CH), 5.242 (t, 1H, *J*= 9Hz), 5.34 (t, 1H, *J*= 10Hz, CH) 5.4 (d, 1H, *J*= 3 Hz, CH). ^{13}C NMR (300MHz, $CDCl_3$): *δ*=20.08, 20.08, 20.1, 20.16, 20.18, 20.35, 20.4 (7x *C*H3CO), 28.25 (*C*H3COS), 30.118 (CH_2CH_2S), 61.1, 62.3, 67.5, 68.03 (CH), 68.65, 68.89, 69.35, 69.56, 69.828(OCH_2CH_2O) 70.08, 71.76, 72.3, 74.87, 95.087 (C1α), 99.92 (C1β), 168.929, 169.212, 169.443, 169.738, 169.931, 170.02, 170.03 (7x CH_3CO), 195(CH_3COS).

Deprotection to give α-D-Mannopyranoside, 2-[2-(2-mercaptoethoxy)ethoxy]ethyl.

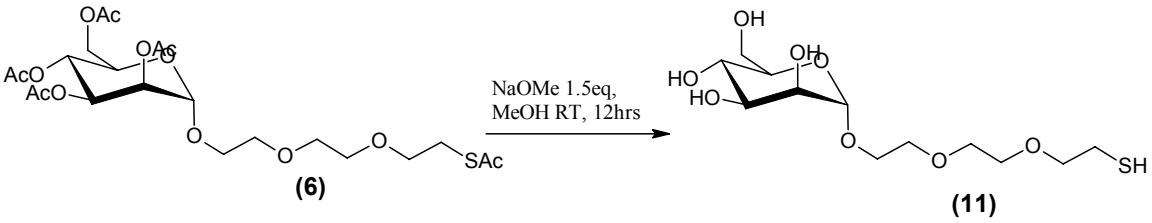

(6) **(11)**

Figure 4S Deacetylation procedure.

α-D-Mannopyranoside, 2-[2-(2-(acetylthio)ethoxy)ethoxy]ethyl,2,3,4,6-tetraacetate (200mg, 0.37 mmol, 1 eq.) was taken and dissolved in anhydrous methanol (5ml). Sodium Methoxide (30 mg 0.055 mmol, 1.5 eq) was added and the solution was stirred at room temperature for 12 hrs. Acidic Ion exchange resin (Amberlite IR-120) was then added and at neutralisation was filtered off and washed

with MeOH. The solvent was then evaporated off to afford the corresponding thiol in high yields (>80%). The initial ^{1}H NMR spectrums indicated the thiol as the main product with disulfide also formed. The amount of disulfide increases over time due to oxidation by atmospheric oxygen. Both thiol and disulfide product forms will interact in the same manner with gold nanoparticles and so no purification is necessary.

α-D-Mannopyranoside, 2-[2-(2-mercaptoethoxy)ethoxy]ethyl **(11)**

^{1}HNMR(300MHz, MeOD, 25°C): *δ*=2.7 (tr, 1H, *J*= 6.6Hz), 2.96 (tr, 1H, *J*= 6.6Hz), 3.6-3.79(m, 10H), 3.8-3.95(m, 4H), 4.0 (dd, 1H, *J*= 3, 1.5Hz, H-2), 4.9 (d, 1H, *J*= 1.5Hz, H-1). ^{13}C NMR (300MHz, MeOD, 25°C): *δ*=24.334, 39.469, 62.387, 67.926, 68.353, 70.485, 71.315, 71.364, 71.538, 71.983, 72.417, 74.433, 101.694. ES-MS calcd. for $C_{12}H_{24}O_8SNa$ $[M+Na]^+$: 351.1090, found 352.0; for $C_{24}H_{45}O_{16}S_2Na$ $[M+Na]^+$ 676.7335, found 676.5. Lit: [6]

β-D-Glucopyranoside, 2-[2-(2-mercaptoethoxy)ethoxy]ethyl **(12)**

^{1}HNMR(300MHz, MeOD, 25°C): *δ*=2.7 (t, 2H, *J*H =6.6Hz), 3.32 (tr, 1H, H-4) 3.4-3.7 (m , 2H, H-5, H-3, H-4), 3.7-3.9 (m, 10H), 3.95 (dd, 1H, *J*=12.3, 2.1Hz, H-2), 4.1 (m, 1H, H-6), 4.52 (d, *J*= 1H, H-1). ^{13}C NMR (300MHz, MeOD, 25°C): *δ*=102.366, 76.096, 76.016, 73.245, 73.144, 71.885, 71.543, 70.588, 69.812, 69.704, 69.480, 69.458, 69.278, 68.599, 67.761, 66.025, 60.751, 37.462, . ES-MS calcd. for $C_{12}H_{24}O_8SNa$ $[M+Na]^+$: 351.1090, found 352.1; for $C_{24}H_{45}O_{16}S_2Na$ $[M+Na]^+$ 676.7335, found 676.5.

β-D-Galactopyranoside, 2-[2-(2-mercaptoethoxy)ethoxy]ethyl **(13)**

^{1}HNMR (300MHz, MeOD, 25°C): *δ*=2.7 (t, 1H, *J*=6.6Hz), 3.6 (dd, 1H, *J*= 10, 8Hz), 3.65-3.9(m, 12H), 3.95 (m, 2H), 4.1 (m, 1H), 4.45 (d, *J*=8Hz, 1H, H-1). ^{13}C NMR (300MHz, MeOD, 25°C): *δ*=23.961, 43.954, 62.786, 67.667, 69.960, 71.082, 71.151, 71.201, 71.442, 72.409, 100.184. ES-MS calcd. for $C_{12}H_{24}O_8SNa$: 351.1090, found 352.1; for $C_{24}H_{45}O_{16}S_2Na$ $[M+Na]^+$ 676.7335, found 676.6. Lit: [6]

β-D-Glucopyranoside, 2-[2-(2-mercaptoethoxy)ethoxy]ethyl 4-O-β-D-galactopyranosyl **(14)**

^{1}HNMR (300MHz, MeOD, 25°C): *δ*=2.8 (t, 2H, *J*=6.6Hz), 3.35 (2H, s), 3.5-3.8 (20H, m), 3.9 (d, 2H, *J*H=3.3Hz, H-4), 4.1 (2H, m), 4.45(d, 1H, *J*H =7.8Hz, H-8 (H-1Gal)), 4.51 (1H, d, *J*H =7.8Hz, H-1Glc). ^{13}C NMR (300MHz, MeOD, 25°C): *δ*=102.54, 101.65, 77.82, 74.88, 73.89, 72.29, 70.41, 69.25, 68.27, 60.6, 59.61, 48.51, 42.79. ES-MS calcd. for $C_{18}H_{34}O_{13}SNa$ $[M+Na]^+$: 513.5198, found 514.4.

β-D-Glucopyranoside, 2-[2-(2-mercaptoethoxy)ethoxy]ethyl 4-O-α-D-glucopyranosyl **(15).**

^{1}HNMR (300MHz, MeOD, 25°C): δ=2.82 (2H, m), 3.25(2H, m), 3.35-4 (20H, m), 4.39(d, 1H, J=7.8Hz, H-1(H-1β-Glu), 5.275(d , 1H, J=3.6Hz, H-1α-Glc). ^{13}C NMR (300MHz, MeOD, 25°C): δ= 102.300, 99.851, 77.176, 76.331, 74.781, 73.198, 73.064, 72.910, 71.889, 69.905, 69.743, 69.553, 68.884, 68.615, 60.967, 60.715, 37.539, 20.574. ES-MS calcd. for $C_{18}H_{34}O_{13}SNa$ $[M+Na]^{+}$: 513.5, found 514.3.

Self-assembly on citrate stabilized particles

$HAuCl_4$ (12.5 mg 0.21mM) was dissolved in H_2O (mQ)(100 ml) and heated to 60°C with constant rapid stirring. Sodium citrate (50 mg, 1.3mM) was dissolved in H_2O (mQ)(50ml) and was also heated to 60 °C upon which it was added to the vigorously stirring gold salt solution in order to keep temperature and concentration variance to a minimum. The temperature was then changed to 85°C and the solution was stirred for another two hours. The initially pale yellow solution gradually turned red indicating colloid formation. The solution was then allowed to cool to room temperature before the next step.

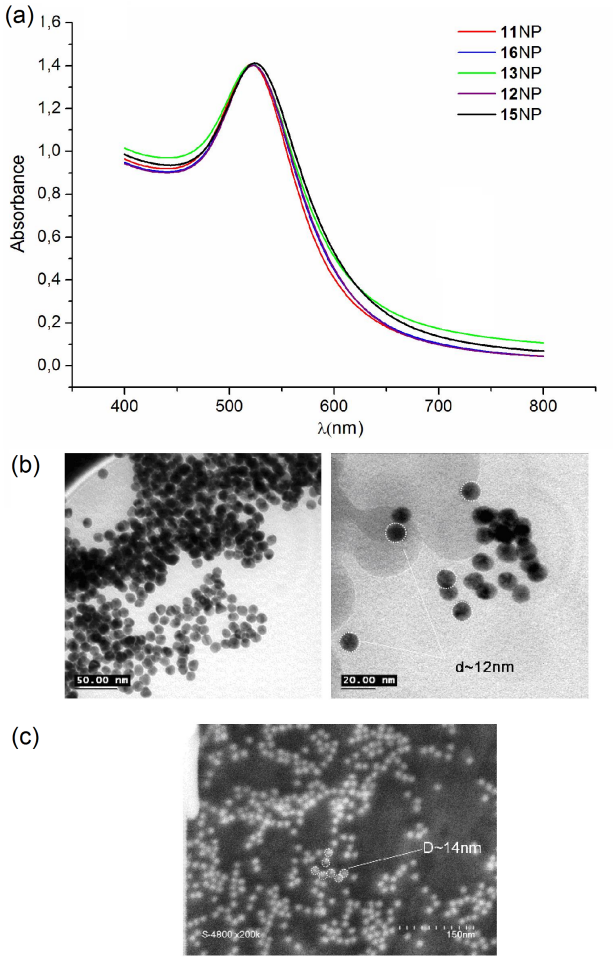

Figure 5S UV-Vis absorption spectra of 8 nM glyconanoparticle solutions, b) TEM and c) SEM and images of mannoside NPs in presence of Con A

To 25 ml of this gold sol (0.21 mM in gold) was added excess of the thiol ligand (50 mg, 6 mM) giving a final ligand to gold ratio of around 30:1. This solution was then allowed to stir at room temperature for 48 hrs before being diluted (x5) with pure water and being centrifuged (14000 r.p.m for 10 minutes) down to remove excess ligand and citrate followed by resuspension in mQ water. This purification procedure was repeated twice followed by resuspension of the particles in Tris buffer. Using this procedure mannoside **(11NP)**, triethyleneglycol **(16NP)**, galactoside **(13NP)**, glucoside **(12NP)** and maltoside **(14NP)** nanoparticles were prepared (Figure 5S).

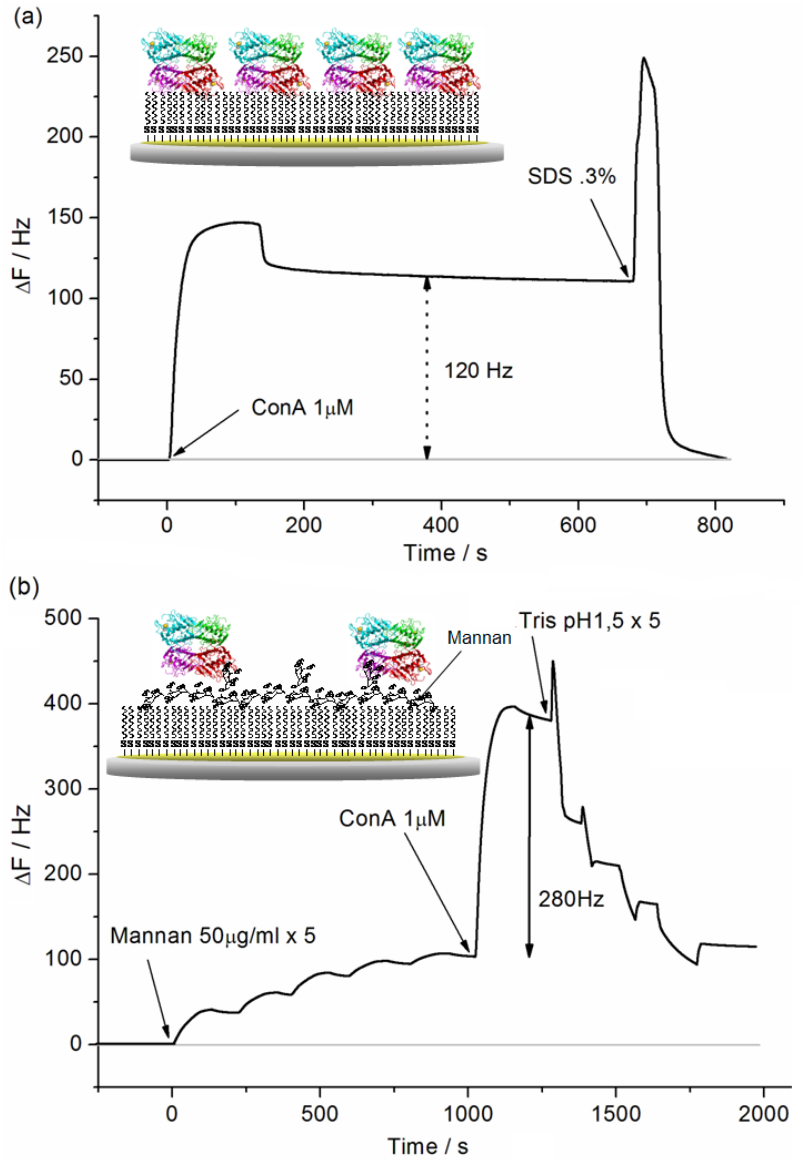

Figure 6S Con A immobilization on a) ODT functionalised gold coated quartz crystal followed by the surface regeneration with SDS solution 0.3% (w/v) and b) ODT/Mannan film to form layer which could be removed through multiple Tris acid buffer injections.

Quartz Crystal Surface Preparation

Hydrophobic self-assembled monolayers were prepared directly on gold coated quartz crystals acquired from Attana. The crystals were firstly immersed in a freshly prepared piranha solution (H_2SO_4 / H_2O_2 7:3) for 1 minute and then washed thoroughly with pure water. They were then dried under a nitrogen stream and immersed in a 1mM octadecanethiol-**ODT** solution (EtOH : Hexane 9:1) for at least 16 hours followed by extensive rinsing with ethanol followed by hexane and then more ethanol and lastly water before being blown dry with a nitrogen stream and being placed in the QCM chip setup.

All QCM experiments were performed at 25°C. Stable layers of Con A were then formed through immobilisation on these octadecanethiol functionalised gold coated crystals from Tris (10 mM) buffered saline (NaCl 0.1M) solutions (Figure 6S). The advantage of this form of immobilisation is its simplicity, allowing an important amount of ConA to be immobilised on the surface (ΔF~120 Hz change in crystals' resonant frequency, corresponding to 84 ng according to the Sauerbrey equation) [25,55] with an ease of surface regeneration apparent using surfactant solution SDS 0.3% w/v (Figure 6Sa).

Specific adsorption through mannoside recognition is another means of Con A immobilisation and can be accomplished with self assembled monolayers (SAMs) or adsorbed films of high specificity. Polysaccharide Mannan adsorbed on polystyrene was demonstrated as an effective Con A immobilisation procedure in experiments by Pei et al.[7] By extension of this procedure the octadecanethiol (ODT) monolayer surface was saturated with the Mannan giving a stable film through repeated injections at a low concentration (50 μg/ml) (Figure 6Sb). Following this Mannan-ODT film deposition passing of buffered Con A solutions at 1 μM concentration resulted in the formation of more dense lectin layers (ΔF~280 Hz change in crystals' resonant frequency, corresponding to 196 ng according to the Sauerbrey equation)[11] which stabilised with time (20-30 minutes). The Mannan-ODT film could be regenerated with multiple injections of buffer at pH 1.5.

UV-VIS Spectroscopy Studies

The gold nanoparticles were prepared as described in the experimental section by a method similar to Russell et al. [8S] These nanoparticles being of optimal size for colorimetric detection were then tested for reversible colorimetric response to selectively recognising lectins. Initially the mannoside functionalised particles were tested for Con A recognition in tris buffered solution (Figure 7S). As described aggregation of nanoparticles based on specific recognition can be measured using UV-optical absorbance. A red-shift in λ_{max} allied to increased intensities at longer wavelengths indicates clustering of nanoparticles to form larger aggregates due to plasmon coupling. It was shown to be concentration as well as time dependant as could be expected. The important thing was that it also proved to be reversible on addition of high-affinity ligand α-1-methyl-D-mannopyranoside indicating specificity (Figure 7S). This technique was also used to validate the galactoside particles which showed a reversible aggregation with the galactospecific RCA120 lectin (Figure 8S).

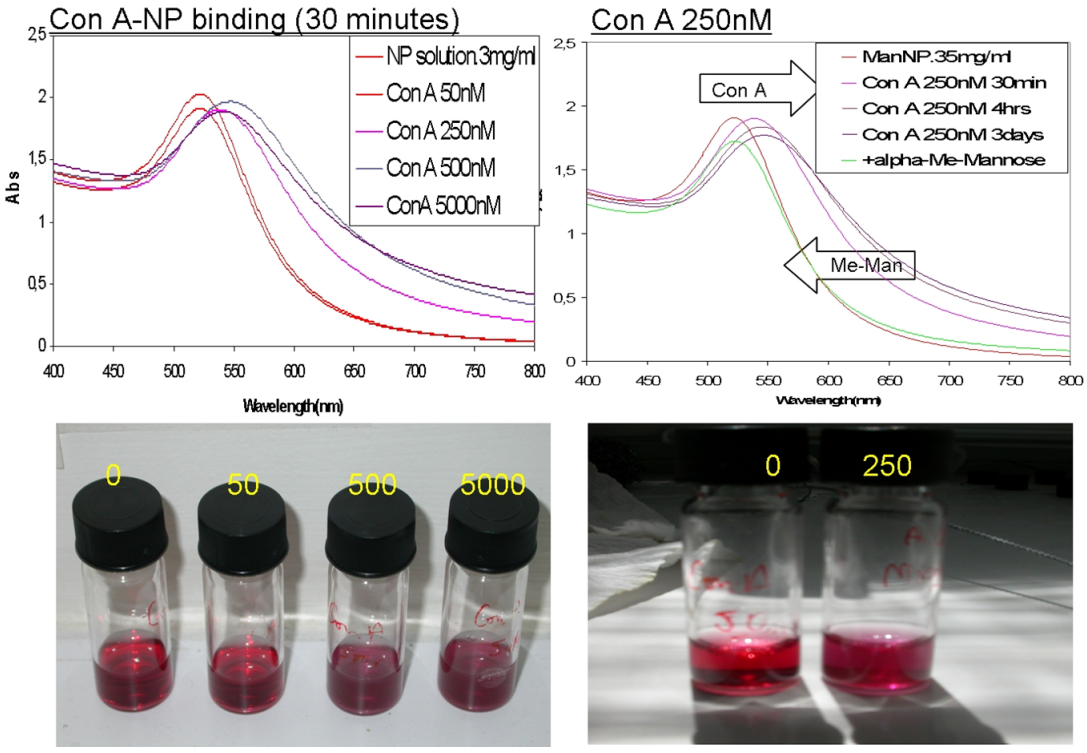

Figure 7S Optical absorption spectroscopy demonstrates reversible Con A driven ManNP agglomeration

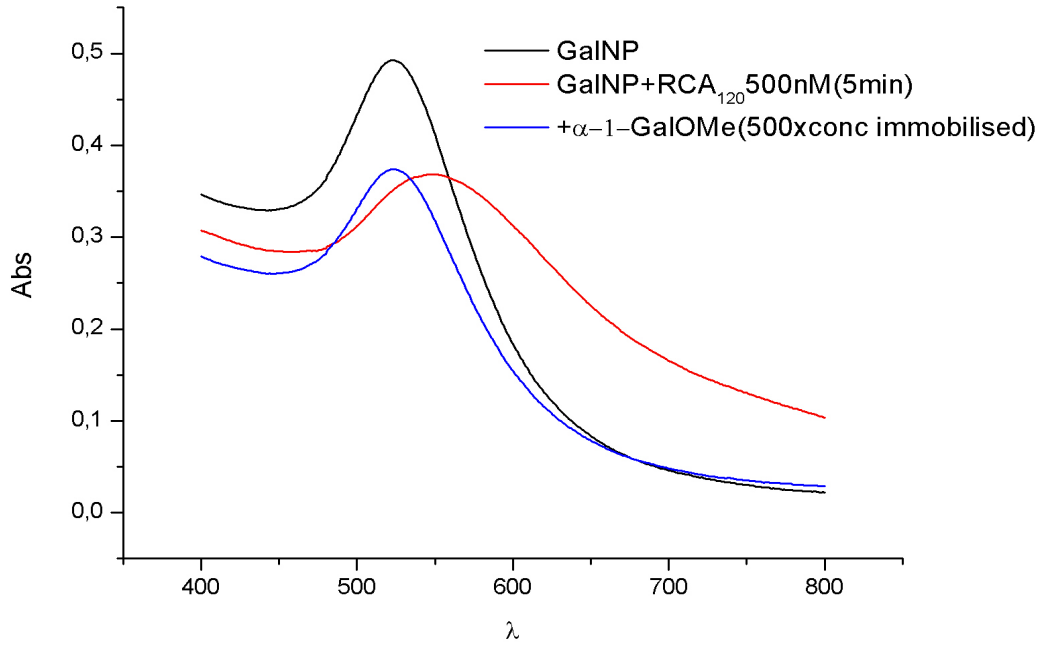

Figure 8S Reversible specific RCA120 recognition by GalNPs

Again aggregation was indicated by an increase in intensity at higher wavelengths which on addition of the α-1-methyl-D-galactopyranoside proved reversible as can be appreciated in the presented graph. Glyconanopartcle suspensions prepared and tested in this manner have been previously demonstrated as colorimetric lectin sensors.[6S,8S]

The concentration of gold cores in the solution could be calculated according to a theoretical study using multipole scattering theory developed by Haiss et al. [9S]

$$N = \frac{A_{450} \times 10^{14}}{d^2\left[-0.295 + 1.36\exp\left(-\left(\frac{d-96.8}{78.2}\right)^2\right)\right]} \qquad (1)$$

Knowing from T.E.M. images that the particle diameter is around 12nm and using the previous equation, where N represents the number density=N/V, nanoparticle molar concentration can be calculated for the NP dispersions.

$$N = A_{450} \text{ x } 5.5745.10^{12}$$

$$N = 5.2265 \text{ x } 10^{12}$$

$$C = N/N_A = 8.679 \text{ x } 10^{-9} \text{ M}$$

The number of ligands per particle can also be estimated assuming complete close-packed monolayer coverage which gives a surface coverage of 196 pmol cm^{-2} .[10S] A 12 nm particle if perfectly spherical would have a surface area of $4.52x10^{-12}$ cm^2 giving $8.85x10^{-10}$ pmol. This number corresponds to 533 thiols per 12 nm particle.

Quartz Crystal Microbalance- QCM biosensors and principles

Surface based systems for biosensing in terms of real-time label-free measurement of biological interactions have been developed which exploit the electro-optical properties of metals (Surface Plasmon Resonance), piezoelectric properties (e) and electrochemical transduction.

The QCM sensors work on the phenomenon of piezoelectricity. This mechanical-electrical effect was first reported in 1880 by the Curie brothers describing the generation of electrical charges on the surface of solids caused by pulling, pushing or torsion. [11S]

While a large number of crystals show piezoelectricity, quartz provides the unique combination of mechanical, electrical, chemical and thermal properties that give it standout applicability. A shear strain is induced in an AT-cut quartz crystal when an alternating current voltage is applied across it through opposing electrodes deposited on its surface. This generates a transversal acoustic wave propagating through the quartz to the contact media. Initially it was demonstrated that there exists a linear relationship between mass adsorbed to crystal surfaces and the crystal's resonant frequency in air or a vacuum[12aS]. Extension of this observation to study biological interactions was realised with the design of solution based systems and combination of these with microfluidics and controlled surface chemistry. Consequently, QCM has become a highly relevant analytical technique due to it sensitive solution-surface interface measurement capability. It possesses a wide detection range which at the low end can detect monolayer coverage by small molecules.

Sauerbrey provided the first treatment of the effect of mass loading on quartz resonators. [12aS] He showed that an ideal layer of foreign mass results in a frequency decrease that is proportional to the deposited mass where the resonator was operated in air or in a vacuum. Assuming the density of the crystal and the adsorbed layer were equal then the following equation applies.

$$\Delta F = \frac{-2f_0^2}{A\sqrt{\mu_q \rho_q}} \Delta m = -S_f \Delta m \qquad (2)$$

f_0 – resonant frequency (Hz)

Δf – frequency change (Hz)

Δm – Mass change (g)

A – peizoelectrically active crystal area (Area between electrodes, m^2)

ρ_q – density of quartz (ρ_q = 2.648 g/cm^3)

μ_q –Shear modulus of quartz for AT-cut crystal ($\mu_q = 2.947 \times 10^{11}$ $g/cm.s^2$)

This equation is valid for a thin, uniform, rigidly attached mass. Application of QCM to biological samples became possible when suitable oscillator circuits for operation in liquids were developed. [12S] As the Sauerbrey relationship was formulated for thin rigid films in air or vacuum questions arose as to the validity of the Sauerbrey relationship in liquid media. For a long time it was postulated that a direct quantification of protein adsorption at functionalised surfaces was possible based on this relationship. However frequency shifts larger than those observed in air were frequently observed in aqueous media for equivalent proteins.

When used in liquid media other important frequency determining factors have to be taken into account such as liquid density and viscosity and the viscosity of the adsorbed materials. These modified resonant frequency shifts were treated theoretically in works such as those by Kanazawa and Gordon [14S] and by Voinova [15-17S].

Although on analysing soft material adsorption in liquid environments the frequency shift cannot be translated directly to mass load according to Sauerbrey relationship, the quartz crystal microbalance can however be used for label free analysis of binding events. Concentration dependant measurements of the frequency shift together with the assumption of a linear relationship between ΔF and Δm allow thermodynamic and kinetic parameters of binding events to be determined as has been demonstrated in numerous examples. Application of QCM to the study of biologically evolved interactions has been

ongoing for the past 20 years. The approaches used for the transduction of biological recognition processes by QCM are enabled through both covalent and physical surface chemistry techniques.

Avidity Constant Estimation. In order to obtain avidity constants of these glyconanoparticles for Con A a concentration assay was run with the results fitted to the Langmuir adsorption Eq. 1:[41]

$$\theta = \frac{K_{eq}[C]}{1 + K_{eq}[C]} \quad (1)$$

Although a simple model it can however be valuable in that it gives access to an equilibrium adsorption constant and so allows the evaluation of surface avidity in at the very least a comparative manner. In terms of QCM measurements ϑ the fractional occupancy can be approximated by $\Delta F / \Delta F_{\max}$ giving

$$\frac{\Delta F}{\Delta F_{\max}} = \frac{K_{eq}[C]}{1 + K_{eq}[C]} \quad (2)$$

which can be rearranged to give :

$$\frac{1}{\Delta F} = \frac{1}{\Delta F_{\max} K_{eq}[C]} + \frac{1}{\Delta F_{\max}} \quad (3)$$

Plotting of $1/\Delta F$ against $1/C$ can give access to the equilibrium adsorption constant K_a (Figure 3c,d). ΔF value measurements were taken just before injection end-equilibrium situation ~125 seconds.

QCM sensing eliminates the need for any labelling step to be part of the signal transduction mechanism. Signal transduction can operate in opaque solutions which may be limiting in optical techniques. The technique is capable of detecting subtle changes at the liquid-surface interface such as density-viscosity changes in the medium, viscoelastic changes in the bound layer and changes in the surface free energy. Also in its favour are its relative ease of use and cost-effectiveness and continually improving sensitivity.

The setup uses a Thickness–Shear–Mode resonator which is composed of an AT-cut quartz crystal sandwiched between two gold electrodes deposited from vacuum. One face of the crystal is in contact with liquid while the other remains in contact with air. The analyte is passed in a continuous flow in the liquid phase (normally buffer) over the functionalised surface and specifically adsorbed mass can be discerned by transduction to an electrical signal as described. This combination of microfluidics and quartz crystal nanobalance allows the real-time label free measurement of molecular interactions. The instrument used was the A100 from Attana Stockholm/Sweden (www.attana.com) where the crystal sensor is setup in a removable holder from which it itself can be removed and chemically modified.

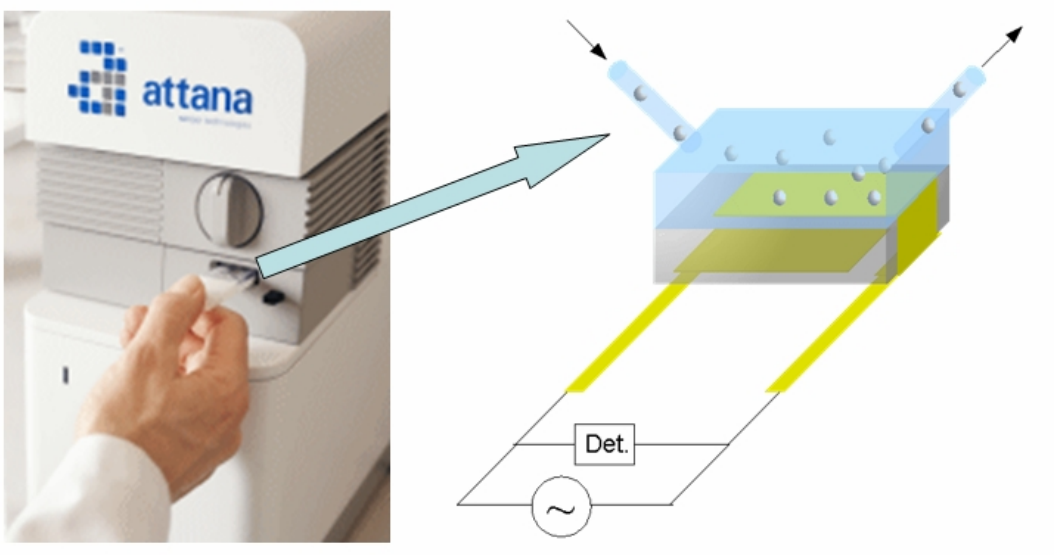

Figure 9S Representation of QCM ATTANA Experimental Setup

Con A Immobilisation Method Dependant Binding

The immobilised lectin layers showed different affinity depending on the immobilisation procedure used (Figure 10S, 11S).

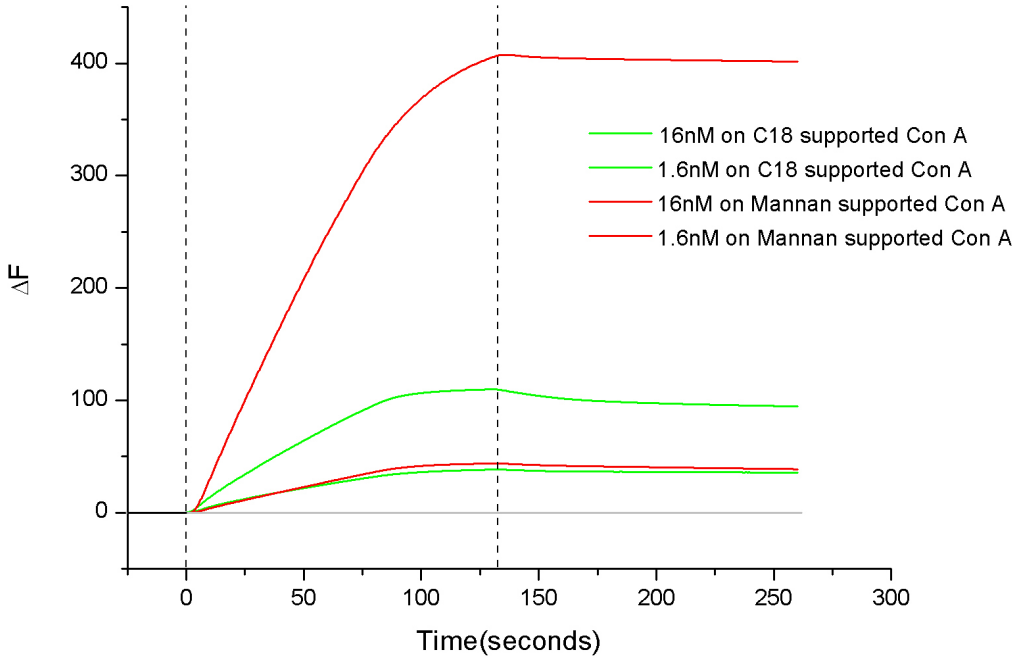

Figure 10S Mannoside nanoparticle injections (16 nM and 1.6 nM in nanoparticles) on immobilised Con A layers.

Con A adsorbed in a specific manner (i.e. on polymannoside) showed increased affinity, which was especially marked in the maltoside nanoparticle case. This could be expected as physical adsorption through the hydrophobic interaction may result in random orientation and have undesired structural effects lowering activity. On the other hand specific adsorption on a Mannan film should result in a more favourable orientation and high activity for the Con A tetramer.

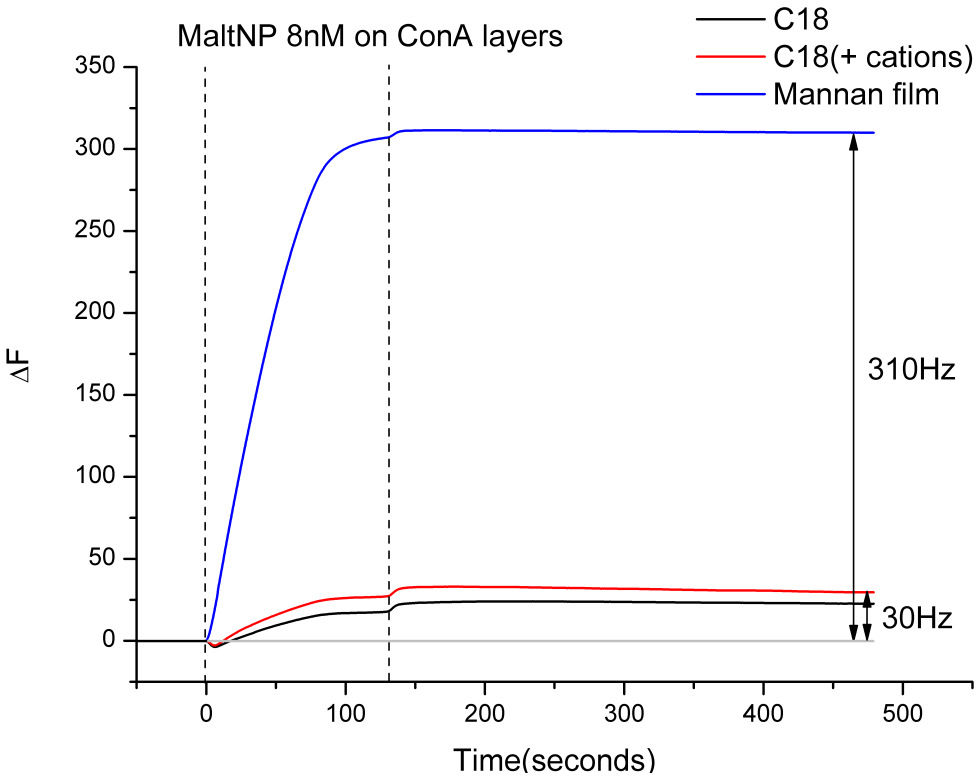

Figure 11S Maltoside nanoparticle injections on immobilised Con A layers.

1S. Woehrle, G. H.; Warner, M. G.; Hutchison, J. E. *Langmuir* **2004,** 20, (14), 5982-5988.
2S. Dahmen, J.; Frejd, T.; Magnusson, G.; Noori, G. *Carbohydrate Research* **1983,** 114, (2), 328-330.
3S. Toshima, K.; Tatsuta, K. *Chem. Rev.* **1993,** 93, (4), 1503-1531.
4S. Milkereit, G.; Gerber, S.; Brandenburg, K.; Morr, M.; Vill, V. *Chemistry and Physics of Lipids* **2005,** 135, (1), 1-14.
5S. Davis, B. G. *J. Chem. Soc.-Perkin Trans. 1* **1999**, (22), 3215-3237.
6S. Schofield, C. L.; Mukhopadhyay, B.; Hardy, S. M.; McDonnell, M. B.; Field, R. A.; Russell, D. A. *Analyst* **2008,** 133, (5), 626-634.
7.S Pei, Z.; Anderson, H.; Aastrup, T.; Ramstroem, O. *Biosensors & Bioelectronics* **2005,** 21, (1), 60-66.
8S. Hone, D. C.; Haines, A. H.; Russell, D. A. *Langmuir* **2003,** 19, (17), 7141-7144.
9S. Haiss, W.; Thanh, N. T. K.; Aveyard, J.; Fernig, D. G. *Analytical Chemistry* **2007,** 79, (11), 4215-4221.
10S. Leff, D. V.; Ohara, P. C.; Heath, J. R.; Gelbart, W. M. *J. Phys.l Chem.* **1995**, *99*, 7036-7041.
11S. Curie, J.; Curie, P. *Comp Rend* **1880,** 91 294–297.
12S. a) Sauerbrey, G. *Zeitschrift Fur Physik* **1959,** 155, (2), 206-222. b) Dunner, G.; Anderson, H.; Mirskog, A.; Hedlund, M.; Astrup, T.; Ramstrom,O. *Langmuir*, **2008**, *24(14)*, 7559-7564; c) Pei, Z.; Anderson, H.; Aastrup, T.; Ramstrom, O. *Biosens. Bioelectron.* **2005**, *21*, 60-66.
13S. Nomura, T.; Okuhara, M. *Analytica Chimica Acta* **1982,** 142, (OCT), 281-284.
14S. Kanazawa, K. K.; Gordon, J. G. *Analytical Chemistry* **1985,** 57, (8), 1770-1771.
15S. Voinova, M. V.; Jonson, M.; Kasemo, B. *Biosensors & Bioelectronics* **2002,** 17, (10), 835-841.
16S. Beck, R.; Pittermann, U.; Weil, K. G. *Journal of the Electrochemical Society* **1992,** 139, (2), 453-461.
17S. Martin, S. J.; Frye, G. C.; Ricco, A. J.; Senturia, S. D. *Analytical Chemistry* **1993,** 65, (20), 2910-2922.